Tomography by Noise

G. Harder,[1] D. Mogilevtsev,[2] N. Korolkova,[3] and Ch. Silberhorn[1,4]

[1]*Applied Physics, University of Paderborn, Warburgerstrasse 100, 33098 Paderborn, Germany*
[2]*Institute of Physics, Belarus National Academy of Sciences, F. Skarina Avenue 68, Minsk 220072 Belarus*
[3]*School of Physics and Astronomy, University of St Andrews, North Haugh, St Andrews KY16 9SS, United Kingdom*
[4]*Max Planck Institute for the Science of Light, Guenther-Scharowsky-Strasse 1/Building 24, 91058 Erlangen, Germany*

We present an efficient and robust method for the reconstruction of photon number distributions by using solely thermal noise as a probe. The method uses a minimal number of precalibrated quantum devices; only one on-off single-photon detector is sufficient. The feasibility of the method is demonstrated by the experimental inference of single-photon, thermal. and two-photon states. The method is stable to experimental imperfections and provides a direct, user-friendly quantum diagnostics tool.

Introduction.—Ultimately, quantum tomography is the most comprehensive tool available for a researcher. Indeed, by inferring the quantum state we have a possibility of predicting results of any possible measurement. From its birth in 1989 [1], quantum tomography has made enormous progress [2,3]. Now even such fragile quantum objects as "Schrödinger cats" made of photons are diagnosed and reconstructed [4]. However, the most precise tool requires the most precise tuning. Generally, quantum reconstruction schemes require precise calibration of the measurement setup together with minimization of noise and losses. For example, one of the most established tomographic tools for electromagnetic field states, quantum homodyne tomography, requires more than 50% overall detection efficiency [5]. Also, rather low respective phase noise of the probe and signal fields is essential for the scheme to work.

In this Letter we present a quantum tomography scheme that actually relies on noise to collect data sufficient for state reconstruction. Furthermore, data are collected by using merely one on-off detector, where the ability to distinguish the number of input photons is not required. The essence of the scheme is simple: the signal mixed with thermal noise impinges on the detector. Varying the intensity of the noise, we can build up the set of measurements sufficient for the inference of diagonal elements of the signal density matrix. The reconstruction can be done even for quite low detection efficiencies on the level of 10%. An important feature of our scheme is the minimization of resources. Even the simplest of conventional schemes using one on-off avalanche photodetector still requires a number of precalibrated absorbers or beam splitters [6]. With increasing signal intensity, this number increases dramatically. Schemes based on time multiplexing or space multiplexing similarly involve a considerable amount of precalibration [7,8]. Additionally, they assume that the signal does not contain photon number contributions beyond the number of multiplexing channels.

In contrast, in our scheme the detector itself can be used to determine the temperature of the noise, thus avoiding the necessity to have any other precalibrated devices. Moreover, there is no restriction to the low dimensional Hilbert space corresponding to the low input photon number predefined by the detector. Our scheme can be generalized to enable a complete reconstruction of the signal state density matrix by mixing the signal with the coherent field.

The scheme.—We first demonstrate the feasibility of our scheme in its simplest configuration. The goal is to infer diagonal elements of the signal density matrix, ρ_{mm}, in the Fock-state basis $|m\rangle$. The probability of registering a signal is generally given as

$$p_j = \sum_{m=0}^{N} \Pi_{jm}\rho_{mm}, \qquad (1)$$

where the elements $\Pi_{jm} = \langle m|\Pi_j|m\rangle$ are related to the jth element of positive valued operator measure (POVM), Π_j, which describes a measurement performed on the signal. $N+1$ is the dimension of the subspace of all possible signal states. We have only one on-off detector and we use different thermal probe states to generate different POVM elements. Let us suppose that the probe completely overlaps with the signal at the detector, which has a detector efficiency η. If we now register "no click" events, we obtain POVM operator matrix elements for such a measurement [9,10],

$$\Pi_{jm} = y_j(1 - y_j\eta)^m, \qquad (2)$$

where $y_j = 1/(1 + \eta n_j)$ and n_j is the mean photon number of the probe thermal state (TS). The matrix with elements $(x_j)^m$ is always nondegenerate for $N+1$ different values of x_j and $m = 0, 1, \ldots, N$ (it is the Vandermonde matrix [11]). Since we can represent the system (1) as $p_j/y_j = \sum_{m=0}^{N}(1 - y_j\eta)^m\rho_{mm}$, it means that using TS

probes provides us with measurements, which should provide enough information to reconstruct elements ρ_{mm}. To collect the necessary data, only one precalibrated on-off detector is needed and it is sufficient to change the probe arbitrarily. When the signal is blocked, the average number of photons n_j in the probe can be measured.

In practice, instead of the simplest scheme (2), we have mixed the probe with the signal using a beam splitter (BS) [see scheme (a) in Fig. (1)]. For two imperfectly overlapping fields, the signal a and the probe b, interfering on the BS and afterwards impinging on the detector, the probability of registering "no click" is given by [12]

$$p_j = \text{Tr}\{: \exp\{-\eta[Ta^\dagger a + (1-T)b^\dagger b + x(a^\dagger b + b^\dagger a)]\} : \rho\sigma_j\}, \quad (3)$$

where $a^\dagger$, a and $b^\dagger$, b are the creation and annihilation operators of the signal and probe modes, σ_j is the density matrix of the jth probe field, T is the transmissivity of the BS, $x = \sqrt{\mu T(1-T)}$, μ is the overlap parameter. and $::$ denotes the normal ordering operator. For perfect overlap, Eq. (3) results in a straightforward relation,

$$\Pi_{jm} = \sum_{n,k,l=0}^{N} (1-\eta)^k \sigma_{nj} |U_{mn}^{kl}|^2. \quad (4)$$

Quantities $\sigma_{nj} = (n_j)^n/(1+n_j)^{n+1}$ are diagonal matrix elements of the jth probe TS. The operator U describes the rotation performed by the BS. It has the following matrix elements in the Fock-state basis:

$$U_{mn}^{kl} = \sqrt{k!l!m!n!} \sum_{g=0}^{k} \sum_{h=0}^{l} \frac{t^{g+h} r^{k+l-g-h}(-1)^{k-g}}{g!h!(k-g)!(h-l)!}$$
$$\times \delta_{m,l+g-h}\delta_{n,k+h-g}. \quad (5)$$

Here $t = \sqrt{T}$ and $r = \sqrt{1-T}$. For zero-temperature noise, $n_j = 0$, Eq. (4) gives

$$p_{\text{signal}} = \sum_{k=0}^{N} (1-T\eta)^k \rho_{kk}. \quad (6)$$

Now let us represent the probe TS as a mixture of coherent states $|\alpha\rangle$ [10]: $\sigma_j = 1/\pi n_j \int d^2\alpha \exp\{-|\alpha|^2/n_j\}|\alpha\rangle\langle\alpha|$. In the case of perfect overlap, p_j for the probe TS can be expressed through the probability of "no clicks" for the coherent probe (given in Ref. [12]),

$$p_j = \frac{1}{\pi n_j} \int d^2\alpha \exp\{-|\alpha|^2/n_j\}$$
$$\times \langle : \exp\{-\eta T(a^\dagger + \nu\alpha^*)(a + \nu\alpha)\} : \rangle_a, \quad (7)$$

where $\nu = \sqrt{(1-T)/T}$. Notice, that this formula is equivalent to the expression for p_j given by POVM elements (4) for $N \to \infty$. The POVM elements for an imperfect overlap can be derived representing Eq. (3) for p_j for the probe TS in a form similar to Eq. (7),

$$p_j = \frac{\bar{n}_j}{\mu n_j} \frac{1}{\pi \bar{n}_j} \int d^2\alpha \exp\{-|\alpha|^2/\bar{n}_j\}$$
$$\times \langle : \exp\{-\eta T(a^\dagger + \nu\alpha^*)(a + \nu\alpha)\} : \rangle_a. \quad (8)$$
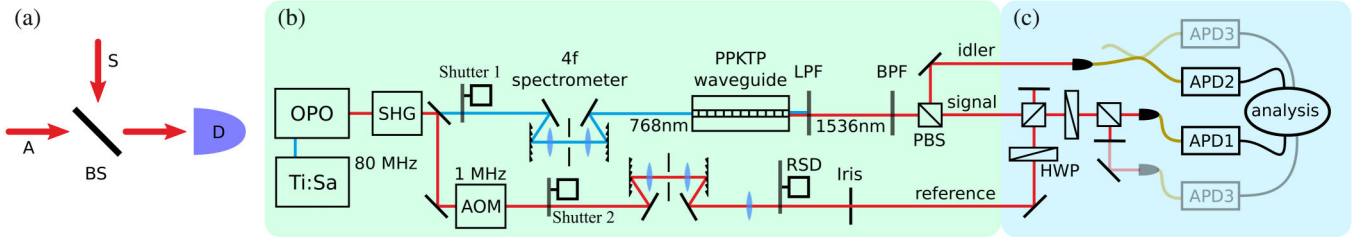

FIG. 1 (color online).   (a) Sketch of the measurement scheme: the signal A is mixed with the probe S on the beam splitter (BS) and impinges on the bucket detector D. (b) State preparation setup. Pulsed light at telecom wavelengths is generated in a Ti:sapphire pumped optical parametric oscillator (OPO) and frequency doubled by second harmonic generation (SHG). Part of the light is separated for later use as a reference field. The repetition rate of the reference is lowered by an acousto-optical modulator (AOM). The 4-f spectrometer tailors the spectral width of the pump beam to achieve spectral decorrelation. The PDC state is generated inside the periodically poled KTP waveguide. The pump is separated by a long pass filter (LPF). A bandpass filter (BPF) is used to suppress background outside the PDC spectrum. Finally the signal and idler are separated at a polarizing beam splitter (PBS). The reference field is also spectrally tailored by a 4-f setup. Pseudothermal light is generated by a rotating speckle disk (RSD) followed by irises. (c) Measurement setup. The power of the reference is controlled by the first half-wave plate (HWP). Signal and reference are overlapped at a PBS-HWP-PBS combination, which effectively constitutes a variable BS adjusted to a splitting ratio of $90:10$. Probed signal and idler are coupled into single mode fibers and impinge onto two avalanche photo diodes (APDs) (Id Quantique id201 at a repetition rate of 1 MHz with a gate width of about 2.5 ns). A third APD is used either in the idler beam to herald two photon states or in the second output port of the variable BS to estimate the mode overlap between the signal and reference by Hong-Ou-Mandel interference.

The quantity $\bar{n}_j = \mu n_j / [1 + (1-\mu)(1-T)\eta n_j]$. Comparing the expression (8) with Eqs. (7) and (4) for perfect overlap, we obtain the relation for the POVM elements in the case of imperfect overlap,

$$\Pi_{jm}^{\text{overlap}} = \frac{\bar{n}_j}{\mu n_j} \sum_{n,k,l=0}^{N} (1-\eta)^k \bar{\sigma}_{nj} |U_{mn}^{kl}|^2, \qquad (9)$$

where $\bar{\sigma}_{nj}$ are the diagonal matrix elements of the TS with the average number of photons $\bar{n}_j$. Equation (9) points to a number of important conclusions. First of all, for zero overlap, the "modified" average number of photons is also zero, $\bar{n}_j = 0$. As follows from Eqs. (6) and (9), the resulting "no click" probability factorizes, $p_j(\mu \to 0) \to p_{\text{signal}} p_{\text{term}}$, where $p_{\text{term}} = 1/[1 + (1-T)\eta n_j]$ is the "no click" probability for the probe TS with vacuum instead of the signal. For a weak probe, when $(1-\mu)(1-T)\eta n_j \ll 1$, the actual situation can be modeled by having two probe modes, the one completely overlapping with the signal with average number of photons equal to μn_j, and the nonoverlapping one with average number of photons equal to $(1-\mu)n_j$. When the probe is strong, $(1-\mu)(1-T)\eta n_j \gg 1$, part of the probe actually interfering with the signal remains constant, $\bar{n}_j \approx \mu/(1-\mu)(1-T)\eta$. In other words, too strong a probe will wash out the effects of interference and destroy the possibility of reconstructing the signal. The optimal regime is moderate levels of the probe TS.

It should be noticed that our setup can be easily generalized for complete state reconstruction. Coherently shifting the signal with amplitude α, one can reconstruct the set of following quantities: $\langle m|D(\alpha)\rho D^\dagger(\alpha)|m\rangle$, where the coherent shift operator is $D(\alpha) = \exp\{\alpha a^\dagger - \alpha^* a\}$. For an N-dimensional density matrix of the signal, it is sufficient to have N different settings of the coherent shift and N TSs to infer the complete density matrix (for the procedure see, for example, Refs. [13]). To realize this generalization with our setup, apart from the one additional fixed BS, one needs only to have a precalibrated phase shifter to change the relative phase of the added coherent field.

Setup.—For the signal state generation we employ a type-II parametric down-conversion (PDC) source in a periodically poled potassium titanyl phosphate (KTP) waveguide. The source is characterized in detail in Ref. [14]. It produces spectrally nearly decorrelated PDC states such that heralded states have a high purity above 80%. Furthermore, being a waveguide source, it allows for efficient coupling into single mode fibers. A scheme of the full setup is shown in Fig. 1. To simulate a noise source with TS photon number statistics, we generate pseudo-thermal light using a rotating speckle disk. For each position of the speckle disk, a random interference pattern is created. After spacial filtering by irises and the final fiber incoupling, the intensity shows an exponential, hence thermal, probability distribution. We verify the thermal statistics by measuring the mean photon number for

different positions of the disk as well as by the second-order correlation function $g^{(2)}$. We obtain $g^{(2)} > 1.9$, whereas a value of $g^{(2)} = 2$ corresponds to perfect thermal statistics and $g^{(2)} = 1$ to Poissonian statistics. The remaining coherent part is thus very small and can be neglected. The calibration parameters of our scheme are the mode overlap between the signal and probe μ and the overall efficiency η. To determine the mode overlap, we adjust our variable beam splitter to 50:50 and measure a Hong-Ou-Mandel dip. The overlap is calculated from the visibility of the dip as described in Ref. [15] to be $\mu = 0.45$. The decrease from unity comes possibly from a spectral mismatch in the 4-f setup or a spacial mismatch while coupling into the fiber. The detection efficiency is measured using the Klyshko scheme [16] from which we obtain $\eta = 0.15$. To generate a set of probe states, we rotate a HWP (see Fig. 1) and measure the mean photon numbers n_j from counts in APD1 with a physically blocked PDC beam.

Results.—Figure 2 shows the results of reconstruction for the heralded single-photon state generated by the scheme depicted in Fig. 1. A total of 150 measurement points were used for the inference. The reconstruction was done using least-squares estimation with non-negativity constraints [17]. The detection efficiency $\eta = 0.15$ and the overlap $\mu = 0.45$ were assumed. Figure 2(d) visualizes the
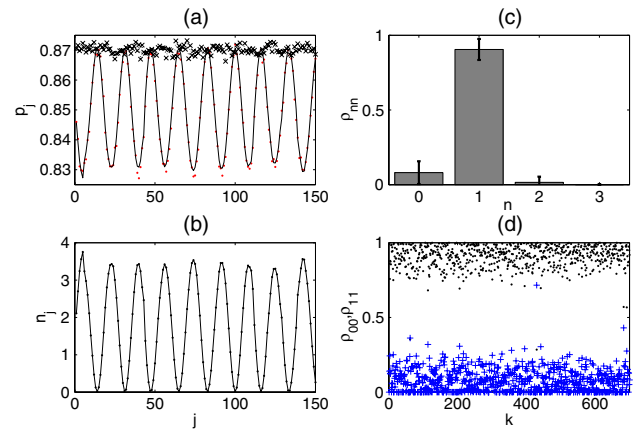

FIG. 2 (color online). Reconstruction of the heralded single-photon state for the scheme parameters $\eta = 0.15$ and $\mu = 0.45$. We used 10^7 PDC pulses for each value of the reference field intensity (a). Dots show experimentally collected data for the number of "no clicks" with respect to the total number of pulses for the signal overlapped with the reference beam. The oscillating behavior comes from the fact that a HWP is used to change the reference beam power at each measurement point. Crosses depict the same probability of "no clicks" on the APD for the signal alone; the solid line shows probabilities estimated by Eq. (9) for the result shown in Fig. 2(c). (b) Average number of thermal photons n_j of the probe for the data of (a). (c) Experimentally inferred ρ_{nn} of the heralded single-photon state. (d) Experimentally estimated values of vacuum (crosses) and single-photon (dots) components of the signal obtained via bootstrapping the data shown in (a).

estimated values of vacuum and single-photon components of the signal obtained via bootstrapping the data [18]. Our reconstruction procedure for the single-photon state gives the following value of the single-photon component: $\rho_{11} \approx 0.905 \pm 0.07$. This estimate conforms well with the result of recent work [14] where the same source was used, demonstrating the high quality of the reconstruction. Also, quite a similar result was obtained with the same source using the "data pattern" reconstruction method [19]. Figure 3 shows experimentally obtained data for the heralded two-photon state and the thermal state [20]. In Fig. 3(a) only part of the measured data are shown. Here, when varying the probe intensity, 600 different values of reference field intensity were taken. The average photon-number distribution shown in Fig. 3(b) is close to the thermal value with the average number of photons equal to 0.17. Relatively large values of variances might be explained by the fact that the signal field intensity was significantly higher compared to the case shown in Fig. 2. As a consequence, parameters of the measurement setup were not as stable. In particular, the detection efficiency was drifting, so that an efficiency drift of about 15% was registered. This deviation might result from a drift in the fiber incoupling efficiency due to instabilities of the setup over the measurement time. The data for the heralded two-photon state are affected in a similar way as can be clearly seen also in Fig. 3(c). Here we
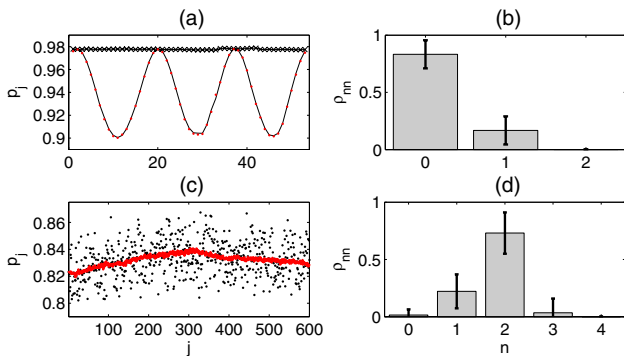

FIG. 3 (color online). (a),(b) Reconstruction of the thermal state. (a) Dots show experimentally collected data for the number of "no clicks" with respect to the total number of pulses for the unheralded signal overlapped with the probe. Crosses depict the relative number of "no clicks" on the APD for the signal alone; the solid line shows probabilities estimated by Eq. (9) for the average reconstruction result shown in Fig. 3(b). (c), (d) Reconstruction of the two-photon state. (c) Dots show experimentally collected data for the number of "no clicks" with respect to the total number of pulses for the heralded two-photon signal without the reference; the solid line shows experimentally collected data for the number of "no clicks" with respect to the total number of pulses for the heralded single-photon signal without the reference. (d) Experimentally inferred ρ_{nn} of the heralded two-photon state obtained accounting for the efficiency drift. The scheme parameters are as in Fig. 2; we took 600 different settings of the reference field.

show experimental data for both the heralded two-photon signal (dots) and heralded single-photon signal (solid line) not mixed with the reference. One of the powerful features of our method is the possibility of accounting for these deviations, by assuming a varying efficiency. For the estimation of the detection efficiency, we need to use the data for the signal state not mixed with the reference. For example, if we take the single-photon state, and use Eq. (6) and the experimentally measured probability p_{signal} as shown in Fig. 2, we can compute the actual values of η. The drift in the detection efficiency η is reflected in the varying value of p_j for the heralded single-photon signal without the reference, as depicted by the solid (red) line in Fig. 3(c). Ideally, this should be a straight line, as it is approximately for the data set with the low field intensity, used for the single-photon state reconstruction (p_j in Fig. 2(a), solid line). For the data set with the higher field intensity, as used for the two-photon reconstruction, this is not the case anymore [Fig. 3(c)]. To account for this, we incorporated the calculated actual efficiency values in the expression for the POVM elements (9) when inferring ρ_{nn} for the generated two-photon state [Fig. 3(d)]. The obtained results for the two-photon signal are quite similar to those obtained recently with the same source using the data pattern method [19]. It should be emphasized that the deviations of the obtained data do not lead to reconstruction artifacts in our scheme. For example, the vacuum component of the reconstructed signal remains very low despite a rather noisy character of the data. Also, the result of reconstruction does unambiguously show that despite low efficiencies of the detection, the scheme produces states with a large two-photon component. All these feature are preserved even if no correction for varying detection efficiency is performed for the two-photon state [Fig. 3(d)], although the relative errors are much higher then.

Conclusions.—We have demonstrated both theoretically and experimentally that reconstruction by noise is indeed feasible and provides a lucid, robust tomographic tool. By merely mixing the signal with the thermal noise and measuring the statistics of the resulting field on the on-off detector, we can collect data sufficient for inferring photon-number distributions of different signal fields. Our reconstruction scheme required only a minimum number of precalibrated devices operating on the single-photon level. For collecting data, only a single on-off detector and a fixed ratio BS were used. The reference field (thermal light) was calibrated using the same detector. Reconstruction of single-photon, thermal, and two-photon states was performed. The scheme has proven to be quite robust with respect to the noise and deviation affecting the measurement setup. Our scheme can be generalized to a complete tomography by adding coherent shifts to the signal. We believe that such a scheme can become a simple, inexpensive, and efficient working tool of quantum diagnostics. Potentially, even spectrally filtered light from such incoherent sources as an incandescent lamp can be used for the probe.

[1] K. Vogel and H. Risken, Phys. Rev. A **40**, 2847 (1989).
[2] *Quantum States Estimation*, edited by M. G. A. Paris and J. Řeháček, Lecture Notes in Physics Vol. 649 (Springer, Berlin, 2004).
[3] See, for example, New J. Phys. **15**, 125020 (2013).
[4] A. Ourjoumtsev, H. Jeong, R. Tualle-Brouri, and P. Grangier, Nature (London) **448**, 784 (2007).
[5] G. M. D'Ariano, U. Leonhardt, and H. Paul, Phys. Rev. A **52**, R1801 (1995).
[6] D. Mogilevtsev, Opt. Commun. **156**, 307 (1998); Acta Phys. Slovaca **49**, 743 (1999).
[7] J. Řeháček, Z. Hradil, O. Haderka, J. Peřina, Jr., and M. Hamar, Phys. Rev. A **67**, 061801(R) (2003); O. Haderka, M. Hamar, and J. Peřina, Jr, Eur. Phys. J. D **28**, 149 (2004).
[8] D. Achilles, Ch. Silberhorn, C. Sliwa, K. Banaszek, and I. A. Walmsley, Opt. Lett. **28**. 2387 (2003).
[9] E. B. Rockower, Phys. Rev. A **37**, 4309 (1988).
[10] J. Peřina, *Quantum Statistics of Linear and Nonlinear Optical Phenomena*, 2nd ed. (Springer; Berlin, 1991).
[11] R. A. Horn and C. R. Johnson, *Topics in Matrix Analysis* (Cambridge University Press. Cambridge, England, 1991), Sec. 6.1.
[12] K. Laiho, M. Avenhaus, K. N. Cassemiro, and Ch. Silberhorn, New J. Phys. **11**, 043012 (2009).
[13] Z. Hradil, D. Mogilevtsev, and J. Řeháček, Phys. Rev. Lett. **96**, 230401 (2006); D. Mogilevtsev, J. Řeháček, and Z. Hradil, Phys. Rev. A **75**, 012112 (2007).
[14] G. Harder, V. Ansari, B. Brecht, Th. Dirmeier, Ch. Marquardt, and Ch. Silberhorn, Opt. Express **21**, 13975 (2013).
[15] K. Laiho, K. N. Cassemiro, and Ch. Silberhorn, Opt. Express **17**, 22823 (2009).
[16] D. N. Klyshko, Sov. J. Quantum Electron. **10**, 1112 (1980).
[17] D. Mogilevtsev, A. Ignatenko, A. Maloshtan, B. Stoklasa, J. Řeháček, and Z. Hradil, New J. Phys. **15**, 025038 (2013).
[18] A simple "jackknife" approach to bootstrapping was used. See, for example, C. F. J. Wu, Ann. Stat. **14**, 1261 (1986). Note that this bootstrapping method has been used in the spirit of minimization of resources, that is, to perform a reliable estimate of the errors and obtain the average values of the density matrix elements while avoiding more cumbersome and advanced methods of statistical analysis [3].
[19] G. Harder, C. Silberhorn, J. Rehacek, Z. Hradil, L. Motka, B. Stoklasa, and L. L. Sanchez-Soto, arXiv:1406.3590v1.
[20] When the idler mode of a single mode PDC state is traced out, the statistics in the signal mode become thermal. Since our PDC source is close to being single mode [14], we expect the statistics to be close to thermal for the unheralded signal.